P- and S-wave velocities of the lowermost crustal rocks from the Kohistan arc: Implications for seismic Moho discontinuity attributed to abundant garnet

Yoshio Kono[*, 1, 3], Masahiro Ishikawa[1], Yumiko Harigane[2], Katsuyoshi Michibayashi[2], Makoto Arima[1]

[1]Graduate School of Environment and Information Sciences, Yokohama National University, 79-7 Tokiwadai, Hodogaya-ku, Yokohama 240-8501, Japan

[2]Institute of Geosciences, Shizuoka University, 836 Ohya, Suruga-ku, Shizuoka 422-8529, Japan

Abstract

P- (Vp) and S-wave (Vs) velocities of garnet-free (two-pyroxene granulite) and garnet-bearing (garnet granulite and garnet pyroxenite) lowermost crustal rocks collected from the Kohistan arc, northern Pakistan, were measured at 0.1-1.0 GPa and 25-400 ˚C. Garnet granulite had higher Vp (+0.31 km/s) and Vs (+0.27 km/s) than two-pyroxene granulite. Although Vp and Vs increased with increasing volume percent of garnet, plagioclase-free garnet pyroxenite showed significantly higher Vp and Vs than plagioclase-rich garnet granulite mainly due to the low Vp and Vs of plagioclase. In contrast, we observed two quasi-linear relationships between Vp (Vs) and SiO_2 content for the garnet-bearing and garnet-free rocks. The garnet-bearing rocks had relatively higher Vp and Vs and stronger SiO_2 dependences than the garnet-free rocks. The stronger SiO_2 dependences of Vp and Vs in the garnet-bearing rocks suggest that the garnet formation in mafic to ultramafic rocks (e.g., pyroxenite and hornblendite), having relatively lower SiO_2,

[*] Corresponding author. Fax: +81 89 927 8405, E-mail: kono@sci.ehime-u.ac.jp (Y. Kono)
[3] Present address: Geodynamics Research Center, Ehime University, 2-5 Bunkyo-cho, Matsuyama 790-8577, Japan

leads to more pronounced increases in Vp and Vs than that of relatively felsic rocks (e.g., felsic-to-mafic granulite). Indeed, the Vp and Vs of the garnet pyroxenite were significantly higher than those of garnet granulite but comparable to those of dunite. The significantly high Vp and Vs of the garnet pyroxenite yielded high reflection coefficients between the garnet granulite and garnet pyroxenite of up to 0.13 for P-waves and 0.14 for S-waves, comparable to values expected for Moho reflection. Thus the lithological boundary between plagioclase-rich garnet granulite and plagioclase-free garnet pyroxenite in the lowermost crust of the Kohistan arc corresponds to the seismic Moho discontinuity.

Keywords: elastic wave velocity, Kohistan, garnet, Moho

1. Introduction

Understanding the structure and composition of island arcs is important to clarifying the nature and growth of the Earth's crust (e.g. Rudnick, 1995; Taylor and McLennan, 1995; Tatsumi, 2005). Seismologically observed seismic wave velocity structures provide important information on the nature of island arcs, in conjunction with experimentally determined P- (Vp) and S-wave (Vs) velocities of crustal rocks (e.g. Christensen and Mooney, 1995; Rudnick and Fountain, 1995). Seismic experiments have been carried out at a number of oceanic island arcs, including the Aleutian (Fliedner and Klemperer, 1999; Holbrook et al., 1999), and Izu-Bonin-Mariana (e.g. Kodaira et al., 2007; Suyehiro et al., 1996; Takahashi et al., 2008) arcs. Various studies have also estimated the crustal structure and composition using the measured and/or calculated Vp and Vs of crustal rocks (e.g. Fliedner and Klemperer, 1999; Holbrook et al., 1999; Kitamura et al., 2003; Tatsumi et al., 2008). A seismic experiment in the Izu-Bonin-Mariana arc showed a Vp of

~6 km/s in the middle crust (Suyehiro et al., 1996); this velocity is comparable to that of tonalite (Kitamura et al., 2003). The presence of an initial continental crust in the middle part of the island arc probably resulted from partial melting of the basaltic lower crust (Nakajima and Arima, 1998). Furthermore, high-density restite, such as garnet-bearing pyroxenite or eclogite, might exist at the base of the island arc, or might be delaminated into the underlying mantle (e.g., Kay and Kay, 1988; 1993; Nakajima and Arima, 1998). Although studies have predicted the existence of such rocks based on seismological observations (e.g. Fliedner and Klemperer, 1998; Tatsumi, 2008), to clarify the structure of the lowermost crust of island arcs, direct experimental investigation of Vp and Vs of arc lowermost crustal rocks are needed.

Previous studies have suggested that the Kohistan terrane in northern Pakistan is an obducted Cretaceous island arc (Kohistan arc) (e.g. Bard et al., 1980; Tahirkheli et al., 1979) that exhibits the lowermost crustal section of the island arc. The seismic structure of the exposed lowermost crustal sections of the Kohistan arc should provide important information for understanding other, less accessible island arcs. The lower crust of the Kohistan arc consists mainly of two-pyroxene granulite and amphibolite, while the lowermost crustal part is composed of garnet-bearing rocks (garnet granulite and garnet pyroxenite) and ultramafic rocks (pyroxenite and dunite). The garnet-bearing assemblage is thought to have formed from a dehydration reaction (Yamamoto and Yoshino, 1998) or by the dehydration-melting (Garrido et al., 2006) of hornblende-bearing mafic to ultramafic rocks. Because garnet has significantly higher Vp and Vs (e.g. Bass, 1989; O'Neill et al., 1989) than other mineral constituents of lower crust such as plagioclase (e.g. Ryzhova, 1964; Seront et al., 1993) and pyroxenes (e.g. Duffy and Vaughan, 1988; Kandelin and Weidner, 1988), the formation of garnet in the lowermost part of the island arc crust significantly affect seismic wave velocity structures. Although previous studies have measured the Vp and Vs of upper to lower crustal rocks (Burlini et al., 2005; Chroston and Simmons, 1989; Miller and Christensen, 1994), they have not focused on the garnet formation in the lowermost crust. To understand the effect of garnet formation on Vp and Vs in the lowermost crust of an island arc, we measured the Vp and Vs of garnet-free (two-pyroxene granulite) and garnet-bearing (garnet granulite and garnet pyroxenite) lowermost crustal rocks from the Kohistan arc, and discuss the seismological structure of the lowermost crust.

2. Regional geology of the Kohistan arc and description of the samples

The lower crust of the Kohistan arc consists of the Chilas complex, the Kamila amphibolite body, and the Jijal complex (Fig. 1a). The Chilas complex and Kamila amphibolite body are mainly composed of two-pyroxene granulite and amphibolite. The Jijal complex, making up the lowermost part of the Kohistan arc, mainly consists of garnet-free and garnet-bearing high-grade metamorphic rocks and ultramafic rocks (pyroxenite and dunite). The upper part of the Jijal complex is composed of two-pyroxene granulite, garnet granulite, and garnet pyroxenite (or garnet hornblendite) (Fig. 1b). Yamamoto and Yoshino (1998) proposed that the garnet granulite was formed from the two-pyroxene granulite by a metamorphic dehydration reaction (plagioclase + orthopyroxene + hornblende = garnet + clinopyroxene + quartz + H_2O). In a recent geochemical study, Garrido et al. (2006) suggested that a dehydration-melting process explains the trace element variations in the two-pyroxene granulite and garnet granulite. They further suggested that dehydration melting of pre-existing hornblendite simultaneously generated the garnet pyroxenite (and garnet hornblendite) in the Jijal complex. In contrast, Garrido et al. (2007) proposed that the Jijal ultramafic rocks (dunite and pyroxenite) were originally mantle peridotite, formed by the reaction of arc melts with subarc mantle peridotite. Previous petrological studies have suggested that the boundary between garnet pyroxenite and granulite facies metamorphic rock (garnet granulite) corresponds to the petrological crust-mantle boundary (e.g. Burg et al., 1998; 2005) (Fig. 1b).

In this study, we examined two-pyroxene granulite (Sample No.: PH332Y, PH335A), garnet granulite (Sample No.: PH332X, PH333D), and garnet pyroxenite (Sample No.: PH330, PH331A). These rock samples were collected in the lower crustal section of the Kohistan arc (Fig. 1a, b). Sample PH335A was collected from the Chilas complex (Fig. 1a), and the other samples were collected from the Jijal complex (Fig. 1b). Table 1 lists modal abundances, chemical compositions of mineral constituents and bulk major element compositions of the rock samples. The modal abundances were counted at 2000 points covering the whole area of a thin section of each sample, and the chemical compositions of minerals were analyzed using an energy-dispersive electron microprobe at Yokohama National University, Japan. The bulk chemical compositions were determined by X-ray fluorescence spectrometry at the National Institute of Polar Research, Japan, with following the analytical procedures of Motoyoshi and Shiraishi (1995).

The two-pyroxene granulite is mainly composed of plagioclase, clinopyroxene and orthopyroxene, and contains minor amounts of hornblende, quartz and ilmenite. Sample PH335A had more plagioclase and less orthopyroxene than sample PH332Y. The two-pyroxenite is bounded by the garnet granulite at the uppermost part of the Jijal complex (Fig. 1b). Samples PH332Y (two-pyroxene granulite) and PH332X (garnet granulite) were collected around the boundary between two-pyroxene granulite and garnet granulite at the uppermost part of the Jijal complex. We observed similar major element compositions between the samples PH332Y and PH332X (Table 1), although the Na_2O content of the samples differed slightly, as also reported by Yamamoto and Yoshino (1998). Garnet granulite is the most abundant rock in the upper part of the Jijal complex (Fig. 1b) and consists mainly of plagioclase, garnet and clinopyroxene with minor amounts of hornblende, quartz and ilmenite. We examined two garnet granulites with different SiO_2 content. Sample PH333D had higher SiO_2 content than sample PH332X (Table 1). In contrast, the garnet pyroxenite does not contain plagioclase and is mainly composed of garnet, clinopyroxene, hornblende and ilmenite. Sample PH330 contained small amounts of garnet (15.13 vol.%), while sample PH331A contained a significant amount of garnet (60.00 vol.%).

The rocks investigated displayed an equigranular texture and had no recognizable linear or planar fabric. Figure 2 shows photomicrographs of the rock samples. The two-pyroxene granulite and garnet granulite each have small grain sizes of ~0.5 mm. In contrast, the garnet pyroxenite exhibits a larger grain size than the two-pyroxene granulite and garnet granulite. The garnet pyroxenite has a maximum grain size of ~1 mm, while almost all of the grains in the garnet pyroxenite are approximately 0.6-0.7 mm. Since the sample volume in our experiment is 1846 mm^3 (14 mm diameter and 12 mm length), each experimental specimen had more than 1000 grains. In addition, the grain sizes of all the samples should have satisfied the required wavelength-grain size relationship. If the wavelength of the elastic wave becomes less than about three times the grain size in the specimen, the energy will be scattered (Mason and McSkimin, 1947). For the frequency of 3 MHz, wavelengths ranged between ~2.3 mm (Vp=~7.0 km/s) and ~2.8 mm (Vp=~8.4 km/s). If we consider the grain size of 0.7 mm, the wavelength is ~3.3-4 times the grain size. Therefore, our samples satisfied the requirement of wavelength/grain size >3.

To confirm the seismic isotropy of the rock samples, we investigated the crystallographic preferred orientation of plagioclase, orthopyroxene, clinopyroxene, and garnet by electron backscattered diffraction at Shizuoka University, Japan, and estimated bulk rock Vp and Vs anisotropies. Figure 3 shows the calculated Vp and faster Vs anisotropies for the rock samples, obtained using the program ANISch5 (Mainprice, 1990). Bulk rock

Vp and Vs were calculated using the Voight-Reuss-Hill average. Variations of elastic constants (Cij) with varying chemical compositions of minerals were calculated by linear interpolation of the Cij values of the end-member minerals. We used Cij data of end-member minerals at ambient conditions, as determined by Seront et al. (1993) for plagioclase, by Jackson et al. (1999) for enstatite, by Bass and Weidner (1984) for ferrosilite, by Levien et al. (1979) for diopside, by Kandelin and Weidner (1988) for hedenbergite, by Sinogeikin and Bass (2000) for pyrope, and by Bass (1989) for grossular and almandine. Figure 3 shows that the rock samples were nearly isotropic except for sample PH330, in which we found slight anisotropy in the Vp and Vs.

3. Vp and Vs measurements

The Vp and Vs measurements were carried out up to 400 ˚C and 1 GPa using a piston-cylinder apparatus (34 mm bore-hole) at Yokohama National University. We used the same experimental cell assembly as used by Kitamura et al. (2003) and Nishimoto et al. (2005). Talc, pyrophyllite and boron nitride (BN) were used as the pressure-transmitting mediums. Each rock specimen (around 14 mm diameter and 12 mm length) was surrounded by BN and talc for quasi-hydrostatically transmitting pressure. Pressure calibration was made using Vp measurements with the high–low quartz transition pressure and temperature at pressures between 0.49 and 1.01 GPa and the temperatures of 694-830 ˚C (see Kono et al., 2007). The uncertainty of the pressure calibration was ±0.03 GPa. In addition, we confirmed that two transitions in NH_4F at room temperature at 0.37 GPa (NH_4F I-II) and 1.17 GPa (NH_4F II-III) (Kuriakose and Whalley, 1968) occured within the error of the pressure calibration. Thus pressure in the Vp and Vs measurements was determined from the load-pressure curve reported by Kono et al. (2007). Temperature was monitored with a Pt-$PtRh_{13}$ thermocouple placed on top of the rock specimen.

The Vp and Vs measurements were carried out using the pulse transmission method. We placed $LiNbO_3$ transducers at both ends of a rock specimen; these transducers had 3 MHz resonant frequency and generate and receive P- (36˚Y-cut) and S-waves (X-cut). The incoming signal and the signal transmitted through the rock specimen were monitored using a digital oscilloscope (HEWLETT-PACKARD: Infinium Oscilloscope 54110A) with a sampling rate of $2\text{x}10^{10}$ sample/second. No band filter or amplifier was used in the experiment. The P- and S-wave travel times were determined by the delay time between the incoming signal and the transmitted signal, with a correction based on travel time for signal path without a sample specimen (cf. Nishimoto et al., 2005). The Vp and Vs measurements had uncertainties of up to ±0.05 and ±0.025 km/s, respectively. The resultant uncertainties in pressure and temperature derivatives of Vp and Vs are ±0.2 km s^{-1} GPa^{-1} for $\partial Vp/\partial P$, ±0.1 km s^{-1} GPa^{-1} for $\partial Vs/\partial P$, $\pm 2.6\text{x}10^{-4}$ km s^{-1} ˚C^{-1} for $\partial Vp/\partial T$, and $\pm 1.3\text{x}10^{-4}$ km s^{-1} ˚C^{-1} for $\partial Vs/\partial T$.

We carried out Vp and Vs measurements up to 1.0 GPa and 400 ˚C at intervals of 0.1 GPa and 100 ˚C. The Vp and Vs measurements were conducted during the depressurization process, because some previous studies reported a hysteresis in the pressure dependence of Vp and/or Vs during pressurization and depressurization, attributed to microcracks which close during pressurization, but do not completely open in the depressurization process (e.g. Burke and Fountain, 1990; Kitamura et al., 2003). We measured the Vp and Vs of the rock samples in the direction parallel to the Y axis, as shown in Fig. 3. Although previous studies measured Vp and Vs along three structural directions (parallel and perpendicular to the lineation and normal to the foliation) for strongly sheared rock samples (Vp and/or Vs anisotropy of more than ~10%) (e.g., Barruol et al., 1992;

Burlini and Fountain, 1993; Ji et al., 1993; Kern and Wenk, 1990), our rock samples showed no recognizable lineation and foliation, and the calculated Vp and Vs exhibited quasi-isotropic Vp and Vs in the rock samples (Fig. 3)

4. General characteristics of Vp and Vs

Table 2 lists the measured Vp, Vs, and pressure and temperature derivatives of Vp and Vs. We estimated Vp and Vs at atmospheric conditions from the Vp and Vs at 1.0 GPa and room temperature and the pressure derivatives of Vp and Vs, and compared the results with those calculated from mineral Cij data by the Voight-Reuss-Hill average (Fig. 3). The Vp and Vs of the two-pyroxene granulites were slightly higher (~2-4 % for Vp and ~1 % for Vs) than those calculated, while the determined Vp and Vs for garnet granulite and garnet pyroxenite were slightly lower (up to ~3 %) than the calculated values. This might have resulted from uncertainties in the Cij data for the end-member minerals; for example, the Cij data for almandine were calculated by linear regression of the Cij-composition relationship to other end-member garnets (Bass, 1989).).

Figure 4 shows Vp and Vs as a function of pressure at 25 ˚C and at various temperatures at 1 GPa for all rock samples. Similar to previous measurements (e.g. Birch, 1960; 1961; Christensen, 1974; Kern, 1990), Vp and Vs increased with increasing pressure (Fig. 4a, c), with significantly increase at 0.1-0.3 GPa followed by linear increase above ~0.4 GPa. Previous studies attributed such significant increase in Vp and Vs to the closure of microcracks at high pressures (e.g. Birch, 1960; 1961; Kern, 1978; Kern and Richter, 1981). Although our Vp and Vs measurements were carried out during the depressurization process, some microcracks might have partially reopened during the depressurization at low pressures. In addition, heating at low pressures might cause thermal cracking. The thermal cracking temperature depends on pressure (about 1 ˚C/MPa) (e.g., Fredrich and Wong, 1986). Therefore, thermal cracking is rare at high pressures, but is more common under low-pressure conditions. This might have caused the marked change in Vp and Vs at pressures lower than 0.3 GPa.

In all the samples, Vp and Vs decreased linearly with increasing temperature as reported by previous studies (e.g., Kern et al., 1999; Khazanehdari et al., 2000) (Fig. 4b, d). We observed marked increase in the temperature derivatives of Vp and Vs with decreasing pressure at 0.4-0.7 GPa (Fig. 5), which might have resulted from the increment of pore volume or thermal cracking in the measured rocks. Thermal cracking is particularly common at low pressures, and could have causes the strong temperature dependences in Vp and Vs at low pressures, as well as the sudden decrease in Vp and Vs at 0.1-0.3 GPa.

5. Discussion

Previous studies have suggested that the garnet-bearing rocks in the lowermost part of the Kohistan arc were formed by either a dehydration reaction (Yamamoto and Yoshino, 1998) or by dehydration melting (Garrido et al., 2006) of pre-existing two-pyroxene granulite and hornblendite. Samples PH332Y (two-pyroxene granulite) and PH332X (garnet granulite) were collected around the lithological boundary and showed similar major element compositions (Table 1). The Vp and Vs results suggest that garnet granulite formation from two-pyroxene granulite causes a marked increase in Vp (+0.31 km/s) and Vs (+0.27 km/s).

Figure 6 shows the Vp and Vs of garnet-bearing rocks as a function of the volume percent of garnet. The data indicate two trends between the Vp (Vs) and the volume percent of garnet, although the chemical compositions of garnets differ among the samples (Table 2). The Vp and Vs estimates for garnet in varying compositions, obtained by linear regression of the Cij data of end-member garnets, show Vp and Vs differences among the garnet rock samples of up to 0.09 and 0.06 km/s, respectively (Fig. 7); these values are comparable to the maximum uncertainties of our Vp and Vs measurements. Therefore, the garnet granulite and garnet pyroxenite exhibit a simple relationship between Vp (Vs) and the volume percent of garnet. We found different trends among the plagioclase-rich garnet granulite and plagioclase-free garnet pyroxenite. The Vp (Vs)-garnet (vol.%) relations of the garnet pyroxenites are comparable to those reported for eclogites (Wang et al., 2005a, b). In contrast, the garnet granulites have lower Vp and Vs than the garnet pyroxenites. This might be attributed to the presence of felsic minerals such as plagioclase, which have significantly lower Vp and Vs (e.g. Ryzhova, 1964; Seront et al., 1993) than mafic minerals (pyroxenes and garnet).

In contrast, the Vp and Vs of the garnet-bearing rocks show a quasi-linear relationship as a function of bulk SiO_2 content. Figure 8 presents the Vp and Vs of garnet-free and garnet-bearing rocks as a function of bulk SiO_2 content. Similar to previous studies (e.g. Rudnick and Fountain, 1995), the Vp and Vs of both garnet-free and garnet-bearing rocks increase with decreasing SiO_2 content. In contrast, we observed two different variations between the garnet-free and garnet-bearing rocks. The garnet-bearing rock has higher Vp values at a given SiO_2 content and stronger SiO_2 dependence than the garnet-free rocks. The Vs-SiO_2 relation also shows different trend between the garnet-bearing and garnet-free rocks (Fig. 8b). The least-square lines for Vp-SiO_2 and Vs-SiO_2 relationships are Vp=-0.0496xSiO_2 (wt.%)+9.523 and Vs=-0.0264xSiO_2 (wt.%)+5.231 for garnet-free rocks, and Vp=-0.0714xSiO_2 (wt.%)+11.066 and Vs=-0.0432xSiO_2 (wt.%)+6.378 for garnet-bearing rocks.

Although Rudnick and Fountain (1995) suggested a simple relationship between Vp and SiO_2 content, the relationship is not simple (Fountain et al., 1990). Fountain (1990) showed strong variations of Vp (~7-8.5 km/s) with SiO_2 content between 43 and 54 wt.%. The strong variations of Vp might be attributed to garnet, as shown in Figure 8. Figure 9 shows Vp, Vs, and SiO_2 relationships for garnet-bearing and garnet-free high-grade metamorphic rocks reported in this study and previous studies (Burke and Fountain, 1990; Fountain et al., 1990; Kern et al., 1996; 1999; Kern and Richter, 1981; Manghnani and Ramananantoandro, 1974; Miller and Christensen, 1994). Similar to Fountain (1990), we observed relatively strong variations in the Vp-SiO_2 and Vs-SiO_2 relationships with SiO_2 content of less than ~50 wt.%, while we found clear trends of markedly higher Vp and Vs in garnet-bearing rocks as compared to garnet-free rocks. The Vp-SiO_2 relationship of the garnet-free rocks is comparable to that determined by Rudnick and Fountain (1995) (Vp = -0.038 x (wt. % SiO_2) + 8.91) (Fig. 9). Although garnet-bearing and garnet-free rocks show comparable Vp and Vs when SiO_2 content is more than ~55 wt.%, the garnet-bearing rocks have higher Vp and Vs and stronger SiO_2 dependences than the garnet-free rocks when SiO_2 content is less than ~50 wt.%, as estimated using only data from the Kohistan arc lower crustal rocks.

These Vp-SiO_2 and Vs-SiO_2 relationships (Figs. 8 and 9) imply that garnet formation has a significant effect on Vp and Vs in mafic to ultramafic rocks with low SiO_2 content. For example, garnet formation in a sample with 55 wt.% SiO_2 content causes only 0.3 and 0.2 km/s increments in Vp and Vs, respectively, while a sample with 45 wt.% SiO_2 content shows significantly higher Vp (+0.6 km/s) and Vs (+0.4 km/s) increments accompanied with garnet formation. The significant increase in Vp and Vs attributed to garnet formation in ultramafic rocks should significantly affect the seismic wave velocity structures of the lowermost arc crust.

Figure 10 presents Vp and Vs at 1.0 GPa and 25 ˚C as functions of density determined under ambient conditions for the major constituents of the Jijal complex. The garnet granulite formation from the two-pyroxene granulite causes increments of Vp (+0.31 km/s), Vs (+0.27 km/s) and density (+0.18 g/cm^3) (Fig. 10), which yield reflection coefficients of 0.05 (P-wave) and 0.06 (S-wave) between the two-pyroxene granulite and garnet granulite. Warner (1990) suggested that seismologically observed lower crustal reflection has a reflection coefficient of 0.1, and therefore replacement from two-pyroxene granulite to garnet granulite will rarely yield seismic reflection in the lower crust.

In contrast, the Vp, Vs, and density of garnet pyroxenite are significantly higher than those of two-pyroxene granulite and garnet granulite, and are comparable to those of dunite. In particular, sample PH331A (3.59 g/cm^3), which contained 60 vol. % of garnet, had a higher density than dunite (3.30 g/cm^3) (Fig. 10). As a result, significantly high reflection coefficients of up to 0.13 for P-waves and 0.14 for S-waves were observed between garnet granulite and garnet pyroxenite. These reflection coefficients are sufficient to cause lower crustal reflection, and are comparable to the seismologically observed Moho reflection of 0.15 (Warner, 1990). Previous studies have also shown significantly high acoustic impedance in eclogites (e.g., Fountain et al., 1994; Kern et al., 1999; Mengel and Kern, 1992), and suggested that existence of eclogite at the base of the crust produces strong reflection at the boundary between overlying crustal rocks (e.g. granulite-facies rocks) and eclogite. Similar to eclogite, the garnet pyroxenites in the lowermost part of the Kohistan arc have significantly high Vp, Vs and density, and also play an important role in producing a seismic Moho reflection similar to eclogite.

Figure 11 shows the reflection coefficient variation in the lowermost part of the Kohistan arc. Miller and Christensen (1994) suggested that the seismic Moho discontinuity is located at the boundary between garnet pyroxenite and ultramafic rocks (dunite and pyroxenite) (Fig. 1b). In contrast, we observed a stronger reflection coefficient between the plagioclase-rich garnet granulite and plagioclase-free garnet pyroxenite. In fact, Miller and

Christensen (1994) also showed significantly high Vp and Vs for garnet hornblendite, but they plotted these high Vp and Vs values in the lithological column of dunite and pyroxenite. These data suggest that the boundary between the plagioclase-rich garnet granulite and plagioclase-free garnet pyroxenite should be the seismic Moho discontinuity of the Kohistan arc, which corresponds to the petrological Moho suggested by Burg et al. (1998).

Since a high-temperature environment is expected at the lowermost part of the arc, it is necessary to discuss the effect of temperature on the difference of Vp and Vs between garnet granulite and garnet pyroxenite. Previous studies found that garnet granulite was metamorphosed at 735-949˚C and 1.0-1.7 GPa (Yamamoto, 1993), and garnet pyroxenite was equilibrated at 800-890 ˚C and 0.8-1.2 GPa (Jan and Howie, 1981). Recent high-temperature Vp and Vs measurements up to 900 ˚C for plagioclase aggregates have indicated strong Vp and Vs reductions above 400 ˚C (Kono et al., 2006; 2008). Therefore, it is possible that plagioclase-rich garnet granulite might show a stronger decrease in Vp and Vs than plagioclase-free garnet pyroxenite under the high-temperature conditions of island arc lowermost crust. Indeed, higher temperature Vp and Vs measurements than those is the present study have revealed that the temperature dependence of Vp and Vs in plagioclase and plagioclase-abundant granulite was comparable to or higher than those of pyroxenite, garnet pyroxenite, and eclogite (e.g., Christensen, 1979; Kern and Richter, 1981; Kono et al., 2004). Therefore, the difference in the Vp and Vs between garnet granulite and garnet pyroxenite under high-temperature conditions in the arc lowermost crust is at least similar to those at room temperature (Figs. 10 and 11) and might be enhanced by the differences in the temperature derivatives of Vp and Vs.

In addition to the strongest reflection coefficient between garnet granulite and garnet pyroxenite, we also found a relatively strong reflection coefficient between garnet pyroxenite and pyroxenite (Fig. 11). Previous studies have also reported that pyroxenites in the Jijal complex have significantly lower Vp and Vs compared to the overlying garnet pyroxenite (Chroston and Simmons, 1989; Kono et al., 2007). We found a maximum reflection coefficient of 0.09 between the garnet pyroxenite and pyroxenite for both P- and S-waves. Such reflection might be observed in the underlying upper mantle. Recent seismological studies of the Izu-Bonin-Mariana arc (Kodaira et al., 2007; Takahashi et al., 2008) have reported upper mantle reflections below the Moho reflection, which might indicate the boundary between garnet-abundant metamorphic rocks and reacted mantle peridotite, such as pyroxenite in the Jijal complex.

Acknowledgements

We thank two anonymous reviewers and the editor for constructive comments and suggestions that improved this manuscript. We are also grateful to H. Yamamoto for his help in the sample collection, and to T. Nakajima and S. R. Khan for their assistance with the fieldwork in 2002 to describe the rock distributions shown in Figure 1b.

References

Bard, J. P., Maluski, H., Matte, Ph., Proust, F., 1980. The Kohistan sequence: crust and mantle of an obducted island arc. Geol. Bull. Univ. Peshawar, Special Issue 13, 87-94.

Barruol, G., Mainprice, D., Kern, H., M. de Saint Blanquat, P. Compte, 1992. 3D seismic study of a ductile shear zone from laboratory and petrofabric data (Saint Barthélémy Massif, northern Pyrénées, France). Terra Nova 4, 63-76.

Bass, J. D., 1989. Elasticity of grossular and spessartite garnets by brillouin spectroscopy. J. Geophys. Res. 94, 7621-7628.

Bass, J. D., Weidner, D. J., 1984. Elasticity of single-crystal orthoferrosilite. J. Geophys. Res. 89, 4359-4371.

Birch, F., 1960. The velocity of compressional waves in rocks to 10 kilobars, part 1. J. Geophys. Res. 65, 1083-1102.

Birch, F., 1961. The velocity of compressional waves in rocks to 10 kilobars, part 2. J. Geophys. Res. 66, 2199-2224.

Burke, M. M., Fountain, D. M., 1990. Seismic properties of rocks from an exposure of extended continental crust-new laboratory measurements from the Ivrea zone. Tectonophysics 182, 119-146.

Burlini, L., Fountain, D. M., 1993. Seismic anisotropy of metapelites from the Ivrea-Verbano zone and Serie dei Laghai (northern Italy). Phys. Earth Planet. Inter. 78, 301-317.

Burlini, L., Arbaret, L., Zeilinger, G., Burg, J. –P., 2005. High-temperature and pressure seismic properties of a lower crustal prograde shear zone from the Kohstan arc, Pakistan. In: Bruhn, D., Burlini, L. (Eds.), High-strain zones: Structure and physical properties. Geol. Soc. London, Spec. Pub. 245, pp. 187-202.

Burg, J. –P., Bondinier, J. –L., Chaudhry, S., Hussain, S., Dawood, H., 1998. Infra-arc mantle-crust transition and intra-arc mantle diapirs in the Kohistan Complex (Pakistani Himalaya): petro-structural evidence. Terra Nova 10, 74-80.

Burg, J. -P., Arbaret, L., Chaudhry, N. M., Dawood, H., Hussain, S., Zeilinger, G., 2005. Shear strain localization from the upper mantle to the middle crust of the Kohistan arc (Pakistan). In: Bruhn, D., Burlini, L. (Eds.), High-strain zones: Structure and physical properties. Geol. Soc. London, Spec. Pub. 245, pp. 25-38.

Christensen, N. I., 1974. Compressional wave velocities in possible mantle rocks to pressures of 30 kilobars. J. Geophys. Res. 79, 407-412.

Christensen, N. I., Fountain, D. M., 1975. Constitution of the lower continental crust based on experimental studies of seismic velocities in granulite. Geol. Soc. Am. Bull. 86, 227-236.

Christensen, N. I., 1979. Compressional wave velocities in rocks at high temperatures and pressures, critical thermal gradients, and crustal low-velocity zones. J. Geophys. Res. 84, 6849-6857.

Christensen, N. I., Mooney, W. D., 1995. Seismic velocity structure and composition of the continental crust: A global view. J. Geophys. Res. 100, 9761-9788.

Chroston, P. N., Simmons, G., 1989. Seismic velocities from the Kohistan volcanic arc, northern Pakistan. J. Geol. Soc. London 146, 971-979.

Duffy, T. S., Vaughan, M. T., 1988. Elasticity of enstatite and its relationship to crystal structure. J. Geophys. Res. 93, 383-391.

Fliedner M. M., Klemperer, S. L., 1999. Structure of an island-arc: wide-angle seismic studies in the eastern Aleutian island, Alaska. J. Geophys. Res. 104, 10667-10694.

Fountain, D. M., Salisbury, M. H., Percival, J., 1990. Seismic structure of the continental crust based on rock velocity measurements from the Kapuskasing uplift. J. Geophys. Res. 95, 1167-1186.

Fountain, D. M., Boundy, T. M., Austrheim, H., Rey, P., 1994. Eclogite-facies shear zones-deep crustal reflectors? Tectonophysics 232, 411-424.

Fredrich, J. T., Wong, T, 1986. Micromechanics of thermally induced cracking in three crustal rocks. J. Geophys. Res. 91, 12743-12764.

Garrido, C. J., Bodinier, J., Burg, J., Zeilinger, G., Hussan, S. S., Dawood, H., Chaudhry, M. N., Gervilla, F., 2006. Petrogenesis of mafic garnet granulite in the lower crust of the Kohistan paleo-arc complex (northern Pakistan): implications for intra-crustal differentiation of island arcs and generation of continental crust. J. Petrol. 47, 1873-1914.

Garrido, C. J., Bodinier, J., Dhuime, B., Bosch, D., Chanefo, I., Bruguier, O., Hussain, S. S., Dawood, H., Burg, J., 2007. Origin of the island arc Moho transition zone via melt-rock reaction and its implications for intracrustal differentiation of island arcs: Evidence from the Jijal complex (Kohistan complex, northern Pakistan). Geol. Soc. Am. 35, 683-686.

Holbrook, W. S., Lizarralde, D., McGeary, S., Bangs, N., Diebold, J., 1999. Structure and composition of the Aleutian island arc and implications for continental crustal growth. Geology 27, 31-34.

Jackson, J. M., Sinogeikin, S. V., Bass, J., 1999. Elasticity of $MgSiO_3$ orthoenstatite. Am. Min. 84, 677-680.

Jan, M. Q., Howie, R. A., 1981. The mineralogy and geochemistry of the metamorphosed basic and ultrabasic rocks of the Jijal complex, Kohistan, NW Pakistan. J. Petrol. 22, 85-126.

Ji, S., Salisbury, M. H., Hanmer, S., 1993. Petrofabric, P-wave anisotropy and seismic reflectivity of high-grade tectonites. Tectonophysics 222, 195-226.

Kandelin, J., Weidner, D. J., 1988. Elastic properties of hedenbergite. J. Geophys. Res. 93, 1063-1072.

Kay, R. W., Kay, S. M., 1988. Crustal recycling and the Aleutian arc. Geochim. Cosmochim. Acta 52, 1351-1359.

Kay, R. W., Kay, S. M., 1993. Delamination and delamination magmatism. Tectonophysics 219, 177-189.

Kern, H., 1978. The effect of high temperature and high confining pressure on compressional wave velocities in quartz-bearing and quartz-free igneous and metamorphic rocks. Tectonophysics 44, 185-203.

Kern, H., Richter, A., 1981. Temperature derivatives of compressional and shear wave velocities in crustal and matle rocks at 6 kbar confining pressure. J. Geophys. 49, 47-56.

Kern, H., 1990. Laboratory seismic measurements: and aid in the interpretation of seismic field data. Terra Nova 2, 617-628.

Kern, H., Wenk, H. –R., 1990. Fabric-related velocity anisotropy and shear wave splitting in rocks from the Santa Rosa mylonite zone, California. J. Geophys. Res. 95, 11213-11223.

Kern, H., Gao, S., Liu, Q. –S., 1996. Seismic properties and densities of middle and lower crustal rocks exposed along the North China Geoscience Transect. Earth Planet. Sci. Lett. 139, 439-455.

Kern, H., Gao, S., Jin, Z., Popp, T, Jin, S., 1999. Petrophysical studies on rocks from Dabie ultrahigh-pressure (UHP) metamorphic belt, Central China: implications for the composition and delamination of the lower crust. Tectonophysics 301, 191-215.

Khazanehdari, J., Rutter, E. H., Brondie, K. H., 2000. High-pressure-high-temperature seismic velocity structure of the midcrustal and lower crustal rocks of the Ivrea-Verbano zone and Serie dei Laghi, NW Italy. J. Geophys. Res. 105, 13843-13858.

Kitamura, K., Ishikawa, M. Arima, M., 2003. Petrological model of the northern Izu-Bonin-Mariana arc crust: constraints from high-pressure measurements of elastic wave velocities of the Tanzawa plutonic rocks, central Japan. Tectonophysics 371, 213-221.

Kodaira, S., Sato, T., Takahashi, N., Ito, A., Tamura, Y., Tatsumi, Y., Kaneda, Y., 2007. Seismological evidence for variable growth of crust along the Izu intraoceanic arc. J. Geophys. Res. 112, B05104, doi:10.1029/2006JB004593.

Kono, Y., Ishikawa, M., Arima M., 2004. Discontinuous change in temperature derivative of Vp in lower crustal rocks. Geophys. Res. Lett. 31, L22601, doi:10.1029/2004GL020964.

Kono, Y., Ishikawa, M., Arima M., 2006. Laboratory measurements of P- and S-wave velocities in polycrystalline plagioclase and gabbronorite up to 700 ˚C and 1 GPa: Implications for the low velocity anomaly in the lower crust. Geophys. Res. Lett. 33, L15314, doi:10.1029/2006GL026526.

Kono, Y., Ishikawa, M., Arima M., 2007. Effect of H_2O released by dehydration of serpentine and chlorite on compressional wave velocities of peridotites at 1 GPa and up to 1000°C. Phys. Earth Planet. Inter. 161, 215-223.

Kono, Y., Miyake, A., Ishikawa, M., Arima M., 2008. Temperature derivatives of elastic wave velocities in plagioclase ($An_{51±1}$) above and below the order-disorder transition temperature. Am. Min. 93, 558-564.

Kuriakose, A. K., Whalley, E., 1968. Phase diagram of ammonium fluoride to 20 kbar. J. Chem. Phys. 48, 2025-2031.

Levien, L., Weidner, D. J., Prewitt, C. T., 1979. Elasticity of diopside. Phys. Chem. Minerals. 4, 105-113.

Mainprice, D., 1990. A fortran program to calculate seismic anisotropy from the lattice preferred orientation of minerals. Computers & Geosciences 16, 385-393.

Manghnani, M. H., Ramananantoandro, R., 1974. Compressional and shear wave velocities in granulite facies rocks and eclogites to 10 kbar. J. Geophys. Res. 79, 5427-5446.

Mason, W. P., McSkimin, H. J., 1947. Attenuation and scattering of high frequency sound waves in metals and glasses. J. Acoust. Soc. Am. 19, 464-473.

Mengel, K., Kern, H., 1992. Evolution of the petrological and seismic Moho-implications for the continental crust-mantle boundary. Terra Nova 4, 109-116.

Miller, D. J., Christensen, N. I., 1994. Seismic signature and geochemistry of an island arc: A multidisciplinary study of the Kohistan accreted terrane, northern Pakistan. J. Geophys. Res. 99, 11623-11642.

Motoyoshi, Y., Shiraishi, K., 1995. Quantitative chemical analyses of rocks with X-ray fluorescence analyzer: (1) Major elements. Nankyoku Siryo (Antarctic Record) 39, 40-48 (in Japanese with English abstract and figure captions).

Nakajima, K., Arima, M., 1998. Melting experiments on hydrous low-K tholeiite: implications for the genesis of tonalitic crust in the Izu-Bonin-Mariana arc. The Island Arc

7, 359-373.

Nishimoto, S., Ishikawa, M., Arima, M., Yoshida, T., 2005. Laboratory measurement of P-wave velocity in crustal and upper mantle xenoliths from Ichino-megata, NE Japan: ultrabasic hydrous lower crust beneath the NE Honshu arc. Tectonophysics 396, 245-259.

O'Neill, B., Bass, J. D., Smyth, J. R., Vaughan, M. T., 1989. Elasticity of a grossular-pyrope-almandine garnet. J. Geophys. Res. 94, 17819-17824.

Rudnick, R. L., 1995. Making continental crust. Nature 378, 571-578.

Rudnick, R. L., Fountain, D. M., 1995. Nature and composition of the continental crust: a lower crustal perspective. Rev. Geophys. 33, 267-309.

Ryzhova, T. V. (1964) Elastic properties of plagioclase. Bull. Acad. Sci. USSR, Geophys. series, 7, 633-635.

Seront, B., Mainprice, D., Christensen, N. I., 1993. A Determination of the three-dimensional seismic properties of anorthosite: Comparison between values calculated from the petrofabric and direct laboratory measurements. J. Geophys. Res. 98, 2209-2221.

Sinogeikin, S. V., Bass, J. D., 2000. Single-crystal elasticity of pyrope and MgO to 20 GPa by Brillouin scattering in the diamond cell, Phys. Earth planet. Inter. 120, 43-62.

Suyehiro, K., Takahashi, N., Ariie, Y., Yokoi, Y., Hino, R., Shinohara, M., Kanazawa, T., Hirata, N., Tokuyama, H., Taira, A., 1996. Continental crust, crustal underplating, and low-Q upper mantle beneath an oceanic island arc. Science 272, 390-392.

Tahirkheli, R. A. K., Mattauer, M., Proust, F., Tapponnier, P., 1979. The India Eurasia suture zone in northern Pakistan: Synthesis and interpretation of recent data at plate scale. In: Farah, A., DeJong, K. A. (Eds.), Geodynamics of Pakistan. Geological Survey of Pakistan, Quetta, pp. 125-130.

Takahashi, N., Kodaira, S., Tatsumi, Y., Kaneda, Y., Suyehiro, K., 2008. Structure and growth of the Izu-Bonin-Mariana arc crust: 1. Seismic constraint on crust and mantle structure of the Mariana arc-back-arc system. J. Geophys. Res. 113, B01104, doi:10.1029/2007JB005120.

Tatsumi, Y., 2005. The subduction factory: How it operates in the evolving Earth. GSA today 15, 4-10.

Tatsumi, Y., Shukuno, H., Tani, K., Takahashi, N., Kodaira, S., Kogiso, T., 2008. Structure and growth of the Izu-Bonin-Mariana arc crust: 2. Role of crust-mantle transformation and the transparent Moho in arc crust evolution. J. Geophys. Res. 113, B02203, doi:10.1029/2007JB005121.

Taylor, S. R., McLennan, S. M., 1995. The Geochemical evolution of the continental crust. Rev. Geophys. 33, 241-265.

Treloar, P. J., Petterson, M. G., Jan, M. Q., Sullivan, M. A., 1996. A re-evaluation of the stratigraphy and evolution of the Kohistan arc sequence, Pakistan Himalaya: implications for magmatic and tectonic arc-building process. J. Geol. Soc. London 153, 681-693.

Yamamoto, H., 1993. Contrasting metamorphic P-T-time paths of the Kohistan granulites and tectonics of the western Himalayas. J. Geol. Soc. London 150, 843-856.

Yamamoto, H., Yoshino, T., 1998. Superposition of replacements in the mafic granulites of the Jijal complex of the Kohistan arc, northern Pakistan: dehydration and rehydration within deep arc crust. Lithos 43, 219-234.

Warner, M., 1990. Absolute reflection coefficients from deep seismic reflections. Tectonophysics 173, 15-23.

Wang, Q., Ji, S., Salisbury, M. H., Xia, B., Pan, M., Xu, Z., 2005a. Pressure dependence and anisotropy of P-wave velocities in ultrahigh-pressure metamorphic rocks from the Dabie-Sulu orogenic belt (China): Implications for seismic properties of subducted slabs and origin of mantle reflections. Tectonophysics 398, 67-99.

Wang, Q., Ji, S., Salisbury, M. H., Xia, B., Pan, M., Xu, Z., 2005b. Shear wave properties and

Poisson's ratio of ultrahigh-pressure metamorphic rocks from Dabie-Sulu orogenic belt, China: Implications for crustal composition. J. Geophys. Res. 110, B08208, doi:10.1029/2004JB003435.

Figure captions

Figure 1. (a) Geological map of the Kohistan arc from Treloar et al. (1996). (b) Route map and sampling points in the Jijal complex with the locations of the petrological Moho (Burg et al., 1998; 2005) and seismic Moho discontinuities suggested by Miller and Christensen (1994) (M&J1994), and this study.

Figure 2. Microphotographs of the measured rock samples. The rock samples show equigranular texture with no recognizable foliation and lineation. Abbreviations: Pl=plagioclase, Opx=orthopyroxene, Cpx=clinopyroxene, Hbl=hornblende, Grt=garnet, Opq=opaque mineral.

Figure 3. Vp (AVp) and faster Vs (AVs) anisotropies calculated from the crystallographic preferred orientation and elastic constants (Cij) of major mineral constituents (plagioclase, orthopyroxene, clinopyroxene, and/or garnet). AVp and AVs are defined as AV=100(Vmax-Vmin)/Vmean. The direction of the Vp and Vs measurement corresponds to the Y direction. The rock samples were quasi-isotropic aggregates except for sample PH330, which had somewhat strong anisotropy.

Figure 4. Vp (a, b) and Vs (c, d) as a function of pressure at 25 ˚C (a, c) and as a function of temperature at 1.0 GPa (b, d). Both Vp and Vs increased with increasing pressure and decreased with increasing temperature.

Figure 5. Temperature derivative of Vp ($\partial Vp/\partial T$) (km s^{-1} ˚C^{-1}) (a) and Vs ($\partial Vs/\partial T$) (km s^{-1} ˚C^{-1}) (b) as a function of pressure. Marked increases in the $\partial Vp/\partial T$ and $\partial Vs/\partial T$ values with

decreasing pressure were obtained at lower pressures than 0.7 GPa.

Figure 6. Vp (a) and Vs (b) at 0.6 GPa and 25 ˚C as a function of volume percent of garnet in the rock samples from the Jijal complex (solid symbols) (from this study and Miller and Christensen, 1994), and those of garnet granulites from other locations (open squares) (Christensen and Fountain, 1975; Manghnani and Ramananantoandro, 1974). The dotted lines represent the linear relationship between Vp (Vs) and volume percent of garnet in eclogite by Wang et al. (2005a) for Vp and Wang et al. (2005b) for Vs, which are comparable to the Vp and Vs results for the garnet pyroxenite. In contrast, plagioclase-rich garnet granulites show lower Vp and Vs than the plagioclase-free garnet pyroxenite.

Figure 7. Change in Vp and Vs with varying chemical compositions of garnet at ambient conditions. End-member garnets have Vp and Vs of 9.32 and 5.49 km/s for grossular (Bass, 1989), of 9.11 and 5.12 km/s for pyrope (Sinogeikin and Bass, 2000), and of 8.42 and 4.74 km/s for almandine (Bass, 1989). The Vp and Vs of garnet solid-solutions were estimated by linear interpolation of those of end-member garnets. Garnets in our rock samples had a comparable Vp and Vs values, with the differences of up to ~0.09 and 0.06 km/s, respectively.

Figure 8. Vp (a) and Vs (b) at 0.6 GPa and 25 ˚C as a function of SiO_2 content for the lower crustal rocks from the Kohistan arc. Solid and broken lines are least square lines for garnet-bearing and garnet-free rocks, respectively. Garnet-bearing rocks have higher Vp and Vs than garnet-free rocks at a given SiO_2 content, and the Vp and Vs difference between garnet-bearing and garnet-free samples increases with decreasing SiO_2 content.

Figure 9. Vp-SiO_2 (a) and Vs-SiO_2 (b) relationships for garnet-bearing and garnet-free high-grade metamorphic rocks reported in this study and previous studies (Burke and Fountain, 1990; Fountain et al., 1990; Kern et al., 1996; 1999; Kern and Richter, 1981; Manghnani and Ramananantoandro, 1974; Miller and Christensen, 1994). The lines represent the least-square lines determined only from the Vp, Vs and SiO_2 data of the garnet-bearing (solid line) and garnet-free (broken line) Kohistan arc lower crustal rocks (Fig. 8) and the calculated Vp-SiO_2 relation of granulites (dotted line) (Rudnick and Fountain, 1995). The Vp-SiO_2 relationship reported by Rudnick and Fountain (1995) is comparable to those of the garnet-free rocks, while the garnet-bearing rocks have higher Vp and Vs when SiO_2 content is less than ~50 wt.%.

Figure 10. Vp (a) and Vs (b) values at 1.0 GPa and 25 ˚C versus density measured at atmospheric conditions for constituents of the Jijal complex. The broken lines are isolines of acoustic impedance. We found significant differences in acoustic impedance between garnet granulite and garnet pyroxenite, which would produce strong reflection at the boundary. The numbers on the symbols represent the data source (1=Kono et al., 2004; 2=Kono et al., 2007; 3=Miller and Christensen, 1994).

Figure 11. Schematic illustration of the lithological column for the Jijal complex and absolute values of the maximum reflection coefficients for P- and S-waves at each lithological boundary. The lithological column was made by considering the route maps in this study (Fig. 1) and in the study by Yamamoto and Yoshino (1998), and the cross section of the Jijal complex described by Burg et al. (2005).

Table 2. P- (Vp) and S-wave (Vs) velocities at 1.0 GPa and 25 ˚C, pressure derivatives of Vp and Vs between 05-1.0 GPa at 25 ˚C, and temperature derivatives of Vp and Vs at 1.0 GPa.

Rock type	Two-pyroxene granulite		Garnet granulite		Garnet pyroxenite	
Sample No.	PH335A	PH332Y	PH332X	PH333D	PH330	PH331A
Vp (km/s)	7.29	7.37	7.68	7.28	7.91	8.37
Vs (km/s)	3.93	3.97	4.24	4.00	4.56	4.72
∂Vp/∂P (km/s GPa)	0.133	0.133	0.038	0.038	0.108	0.030
∂Vs/∂P (km/s GPa)	0.021	0.032	0.036	0.032	0.020	0.001
∂Vp/∂T (km/s ˚C)	-1.3×10^{-4}	-0.3×10^{-4}	-1.2×10^{-4}	-2.2×10^{-4}	-2.3×10^{-4}	-1.5×10^{-4}
∂Vs/∂T (km/s ˚C)	-0.9×10^{-4}	-0.4×10^{-4}	-0.9×10^{-4}	-0.9×10^{-4}	-0.5×10^{-4}	-0.8×10^{-4}

Table 1. Modal abundance, chemical composition of major mineral constituents and bulk chemical composition of rock samples

Rock type	Two-pyroxene granulite		Garnet granulite		Garnet clinopyroxenite	
Sample No.	PH335A	PH332Y	PH332X	PH333D	PH330	PH331A
Mode (vol.%)						
Garnet	-	-	36.80	23.50	15.13	60.00
(Ca:Mg:Fe)			(0.24:0.35:0.41)	(0.18:0.34:0.48)	(0.25:0.38:0.37)	(0.19:0.46:0.35)
Orthopyroxene	11.79	19.20	-	-	-	-
(Mg:Fe)	(0.65:0.35)	(0.60:0.40)				
Clinopyroxene	19.87	20.00	21.80	25.50	81.07	33.45
(Mg:Fe)	(0.75:0.25)	(0.63:0.37)	(0.75:0.25)	(0.72:0.28)	(0.85:0.15)	(0.83:0.17)
Hornblende	2.62	2.60	0.20	1.00	3.00	5.65
Plagioclase	63.54	53.60	36.00	43.00	-	-
(Ca:Na)	(0.58:0.42)	(0.59:0.41)	(0.54:0.46)	(0.38:0.62)		
Quartz	1.09	2.10	3.00	5.00	-	-
Ilmenite	1.09	2.50	2.20	2.00	0.80	0.90
Oxide (wt.%)						
SiO_2	48.94	48.19	49.17	51.85	47.57	41.19
TiO_2	0.55	0.82	0.82	0.98	0.49	0.34
Al_2O_3	16.70	17.05	17.84	17.06	6.58	16.06
Fe_2O_3	9.48	11.88	11.82	9.31	8.04	15.72
MnO	0.15	0.20	0.19	0.14	0.12	0.38
MgO	7.38	5.87	5.79	4.78	13.30	12.45
CaO	10.98	10.59	10.95	10.40	21.17	12.09
Na_2O	2.24	2.38	1.46	2.58	0.28	0.02
K_2O	0.16	0.16	0.13	0.26	0.00	0.00
P_2O_5	0.00	0.06	0.03	0.10	0.00	0.00
total	96.58	97.54	98.20	97.46	97.19	96.57

Ratio in parenthesis represents chemical composition of major mineral constituents (garnet, orthopyroxene, clinopyroxene, plagioclase).

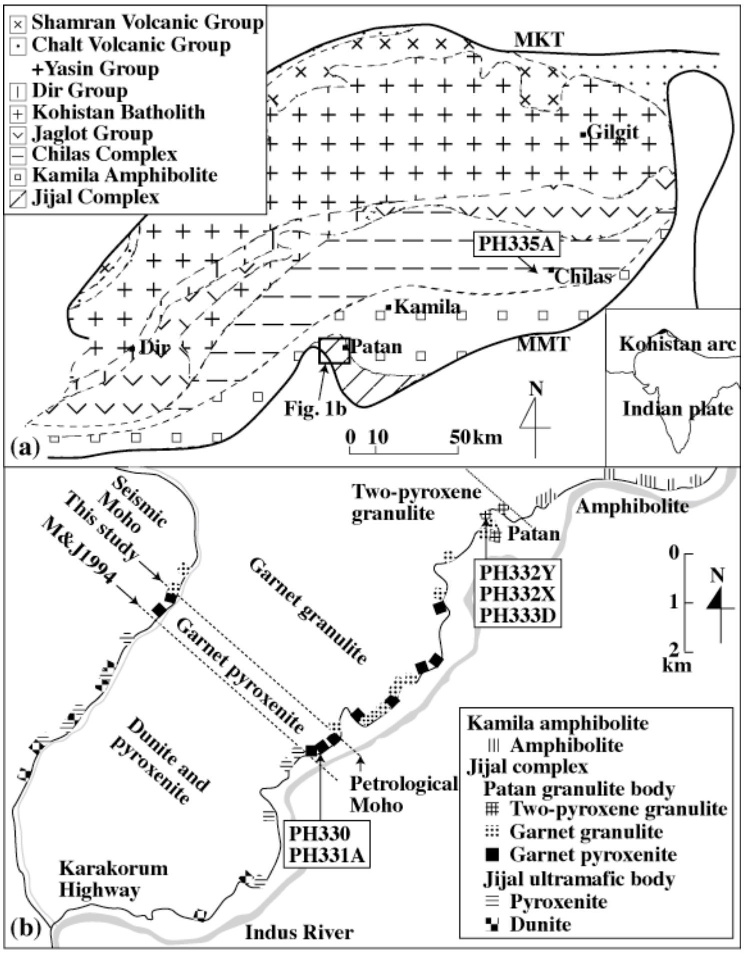
Shamran Volcanic Group
Chalt Volcanic Group
+Yasin Group
Dir Group
Kohistan Batholith
Jaglot Group
Chilas Complex
Kamila Amphibolite
Jijal Complex
MKT
Gilgit
PH335A
Chilas
Kamila
Patan
MMT
Dir
Fig. 1b
N
0 10 50km
Kohistan arc
Indian plate
(a)
Seismic Moho
This study
M&J1994
Two-pyroxene granulite
Patan
Amphibolite
PH332Y
PH332X
PH333D
Garnet granulite
Garnet pyroxenite
Dunite and pyroxenite
Petrological Moho
PH330
PH331A
0
1
2
km
N
Kamila amphibolite
Amphibolite
Jijal complex
Patan granulite body
Two-pyroxene granulite
Garnet granulite
Garnet pyroxenite
Jijal ultramafic body
Pyroxenite
Dunite
Karakorum Highway
Indus River
(b)

Figure 1

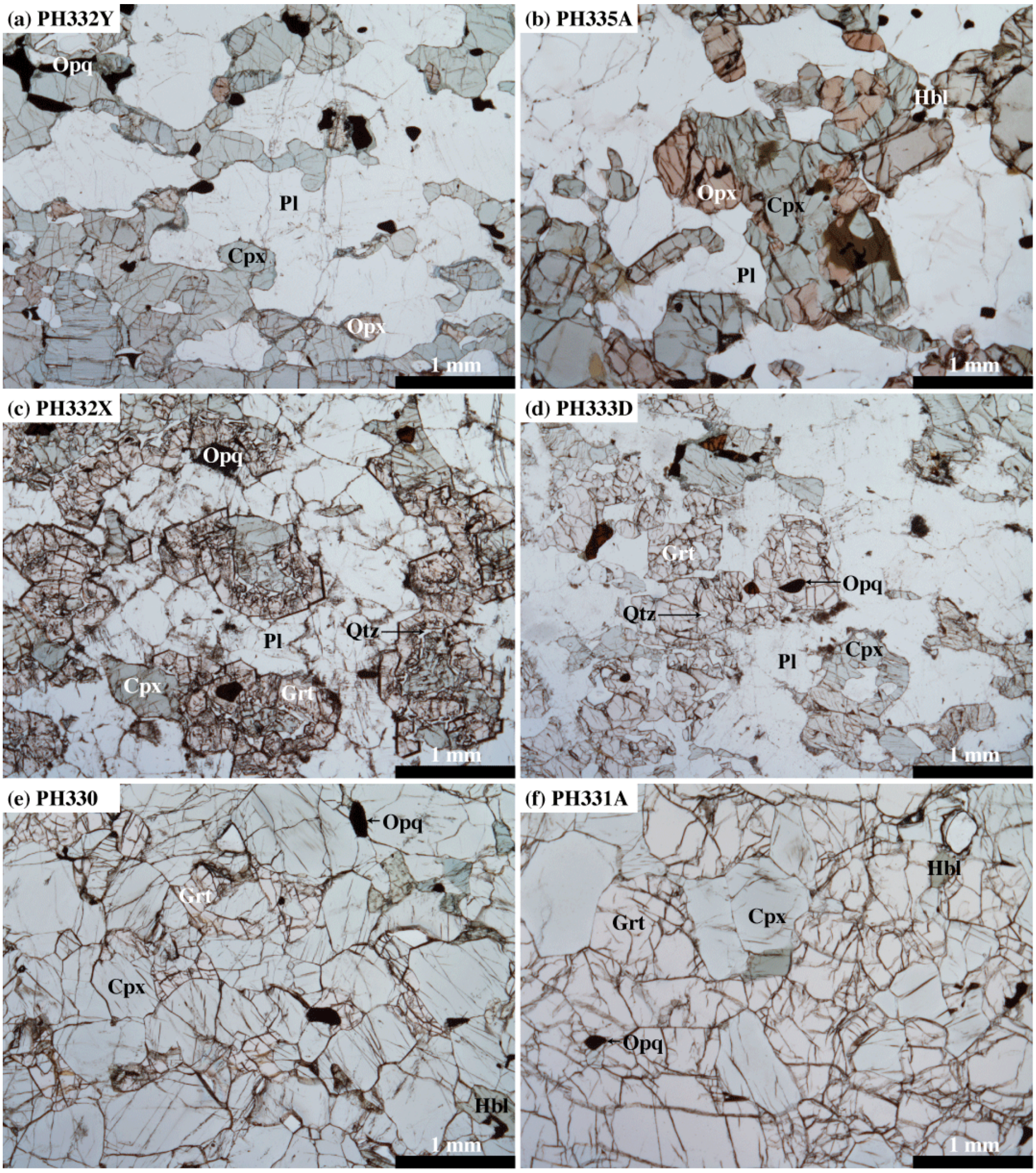

(a) PH332Y
Opq
Pl
Cpx
Opx
1 mm
(b) PH335A
Hbl
Opx
Cpx
Pl
1 mm
(c) PH332X
Opq
Pl
Qtz
Cpx
Grt
1 mm
(d) PH333D
Grt
Opq
Qtz
Pl
Cpx
1 mm
(e) PH330
Opq
Grt
Cpx
Hbl
1 mm
(f) PH331A
Hbl
Grt
Cpx
Opq
1 mm

Figure 2

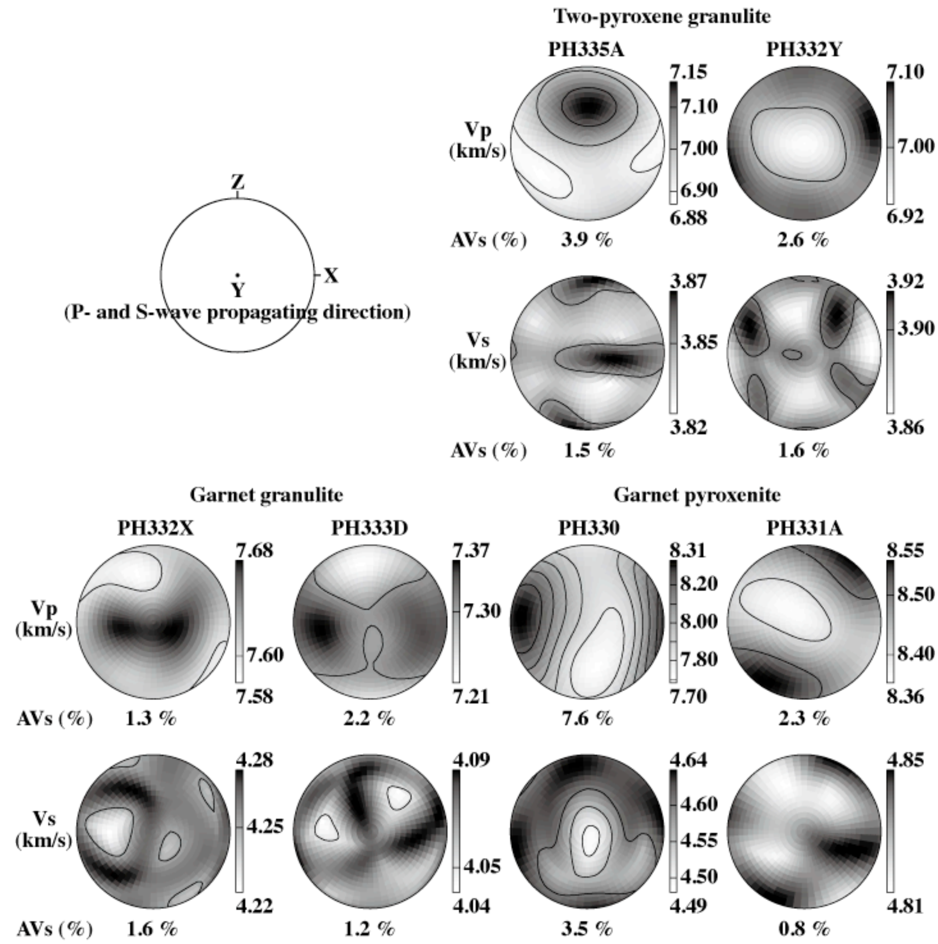

Z
X
Y
(P- and S-wave propagating direction)
Two-pyroxene granulite
PH335A
PH332Y
Vp
(km/s)
7.15
7.10
7.00
6.90
6.88
7.10
7.00
6.92
AVs (%)
3.9 %
2.6 %
Vs
(km/s)
3.87
3.85
3.82
3.92
3.90
3.86
AVs (%)
1.5 %
1.6 %
Garnet granulite
Garnet pyroxenite
PH332X
PH333D
PH330
PH331A
Vp
(km/s)
7.68
7.60
7.58
7.37
7.30
7.21
8.31
8.20
8.00
7.80
7.70
8.55
8.50
8.40
8.36
AVs (%)
1.3 %
2.2 %
7.6 %
2.3 %
Vs
(km/s)
4.28
4.25
4.22
4.09
4.05
4.04
4.64
4.60
4.55
4.50
4.49
4.85
4.81
AVs (%)
1.6 %
1.2 %
3.5 %
0.8 %

Figure 3

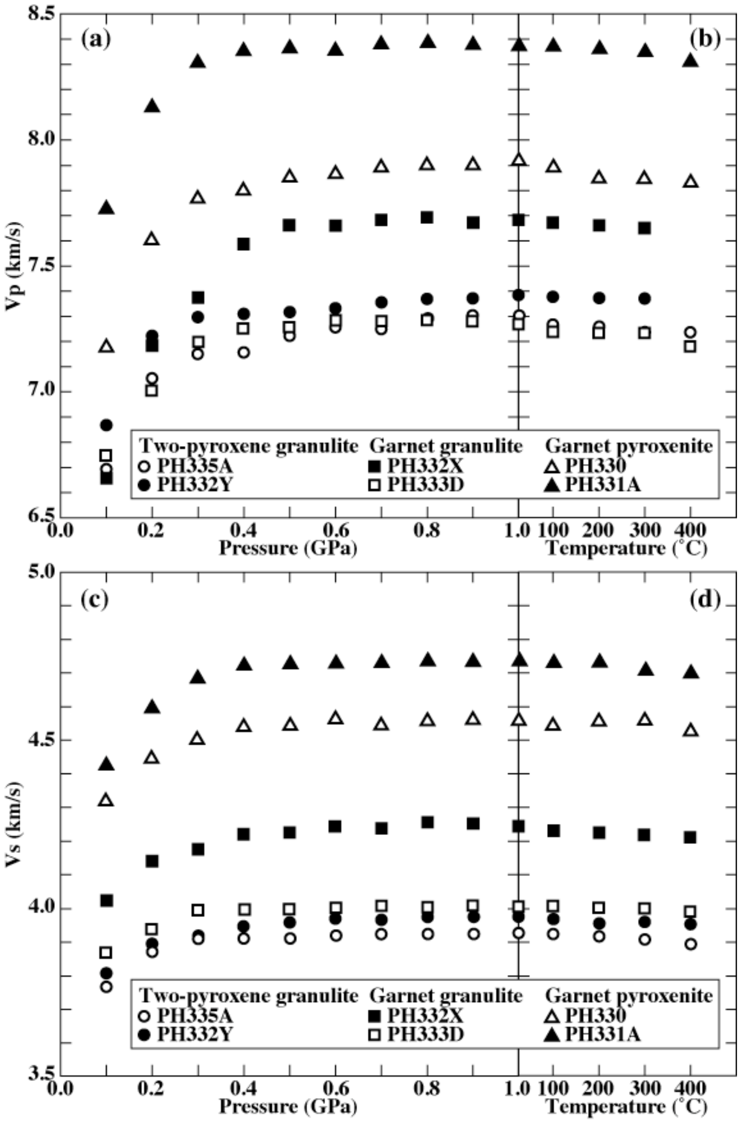

(a)
(b)
(c)
(d)
Vp (km/s)
Vs (km/s)
Pressure (GPa)
Temperature (°C)
Two-pyroxene granulite
PH335A
PH332Y
Garnet granulite
PH332X
PH333D
Garnet pyroxenite
PH330
PH331A

Figure 4

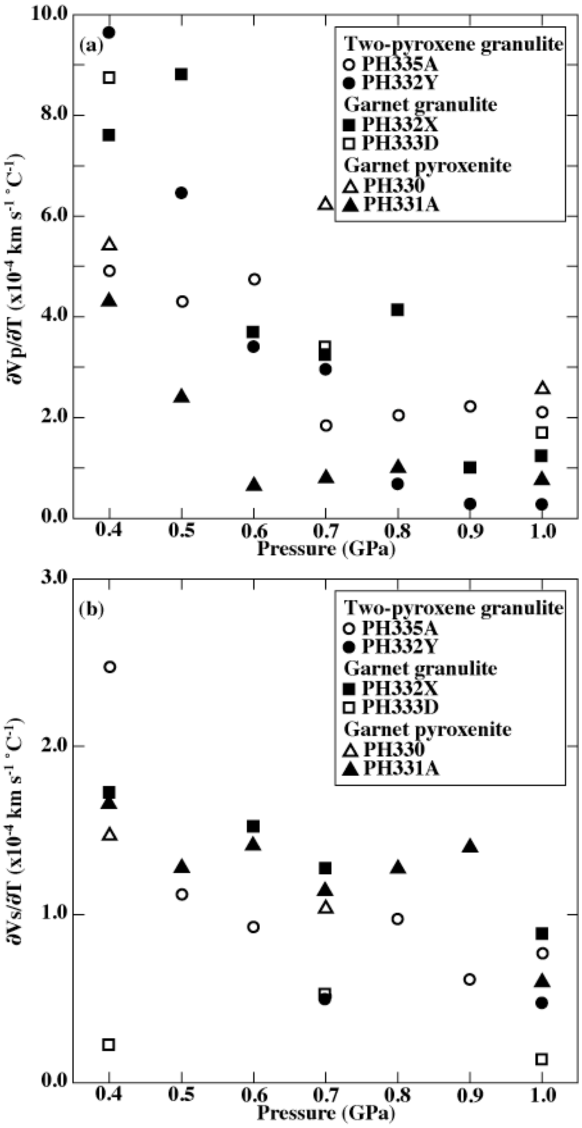

(a)
Two-pyroxene granulite
PH335A
PH332Y
Garnet granulite
PH332X
PH333D
Garnet pyroxenite
PH330
PH331A
∂Vp/∂T (x10⁻⁴ km s⁻¹ °C⁻¹)
Pressure (GPa)
(b)
Two-pyroxene granulite
PH335A
PH332Y
Garnet granulite
PH332X
PH333D
Garnet pyroxenite
PH330
PH331A
∂Vs/∂T (x10⁻⁴ km s⁻¹ °C⁻¹)
Pressure (GPa)

Figure 5

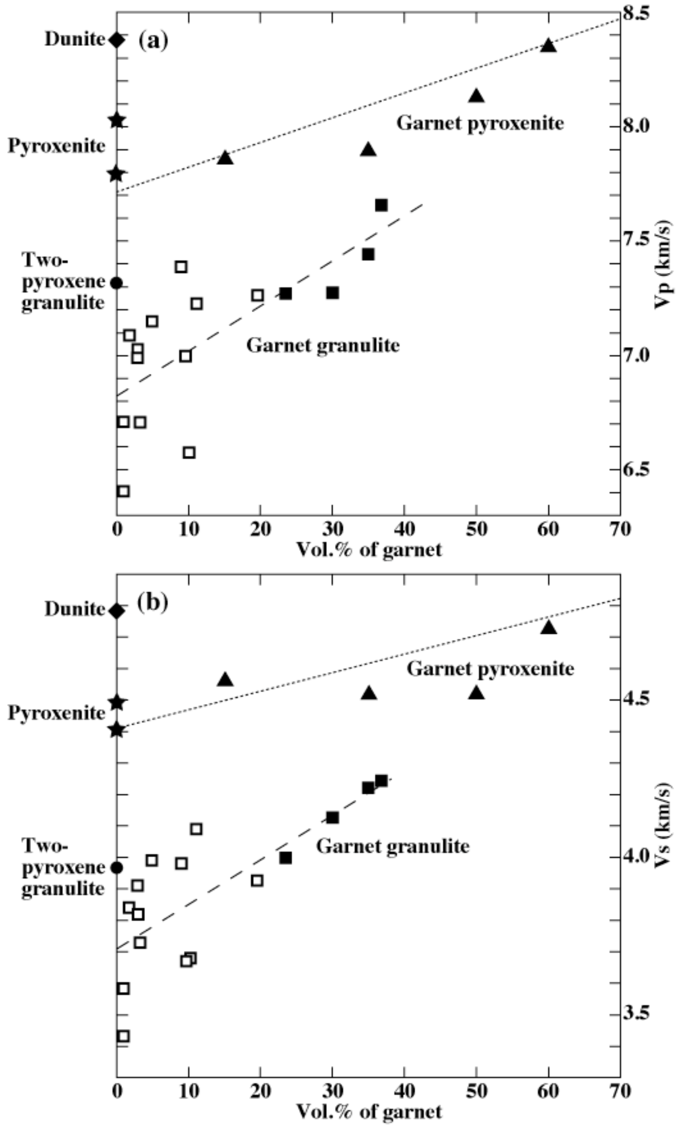
Dunite
(a)
Pyroxenite
Garnet pyroxenite
Two-
pyroxene
granulite
Garnet granulite
Vp (km/s)
8.5
8.0
7.5
7.0
6.5
0
10
20
30
40
50
60
70
Vol.% of garnet
Dunite
(b)
Pyroxenite
Garnet pyroxenite
Two-
pyroxene
granulite
Garnet granulite
Vs (km/s)
4.5
4.0
3.5
0
10
20
30
40
50
60
70
Vol.% of garnet

Figure 6

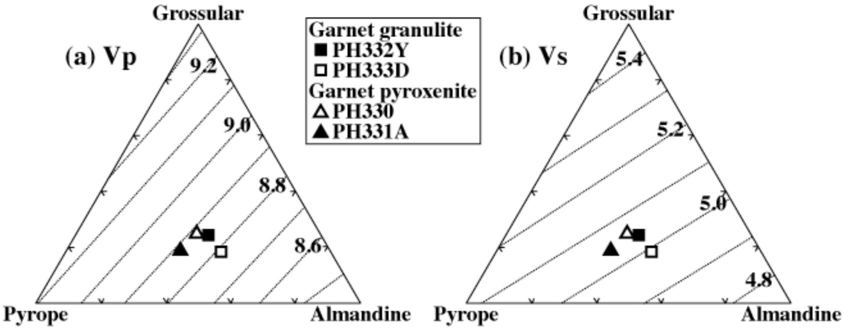
Grossular
(a) Vp
9.2
9.0
8.8
8.6
Pyrope
Almandine
Garnet granulite
PH332Y
PH333D
Garnet pyroxenite
PH330
PH331A
Grossular
(b) Vs
5.4
5.2
5.0
4.8
Pyrope
Almandine

Figure 7

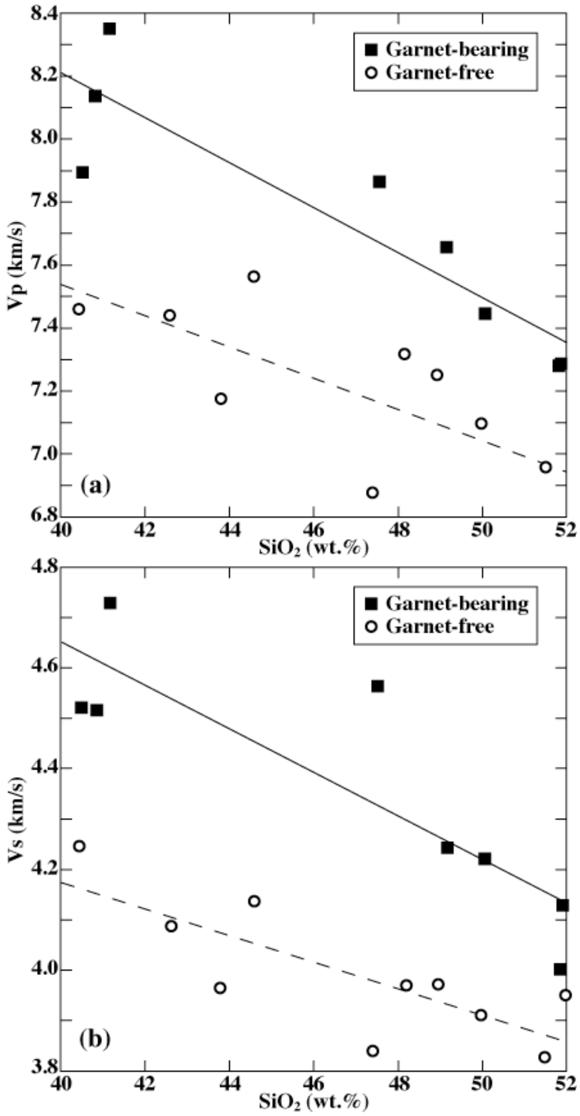

Garnet-bearing
Garnet-free
Vp (km/s)
(a)
SiO2 (wt.%)
Garnet-bearing
Garnet-free
Vs (km/s)
(b)
SiO2 (wt.%)

Figure 8

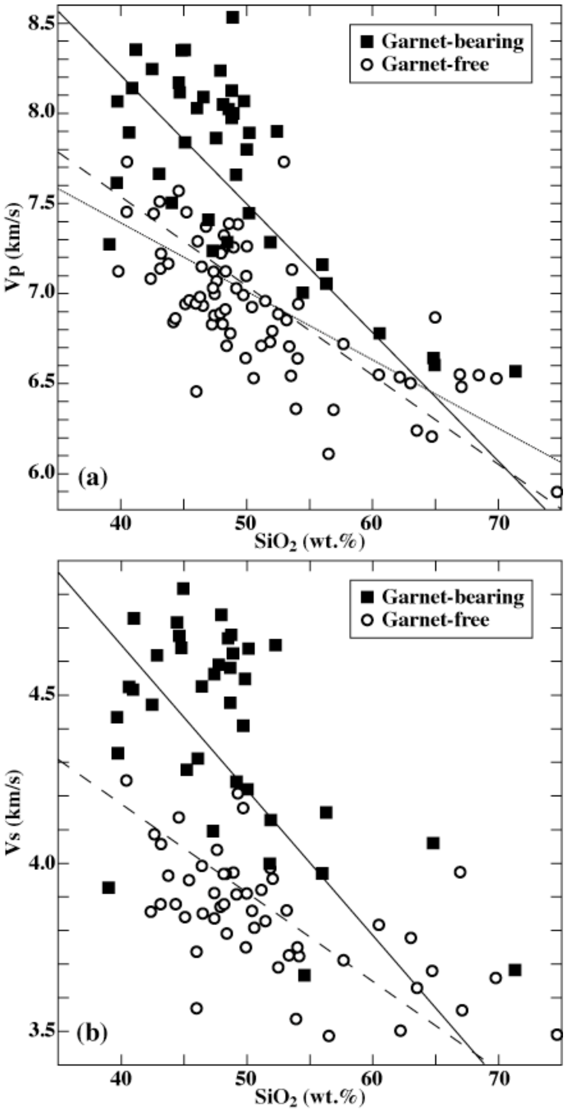
Garnet-bearing
Garnet-free
Vp (km/s)
8.5
8.0
7.5
7.0
6.5
6.0
(a)
40
50
60
70
SiO2 (wt.%)
Garnet-bearing
Garnet-free
Vs (km/s)
4.5
4.0
3.5
(b)
40
50
60
70
SiO2 (wt.%)

Figure 9

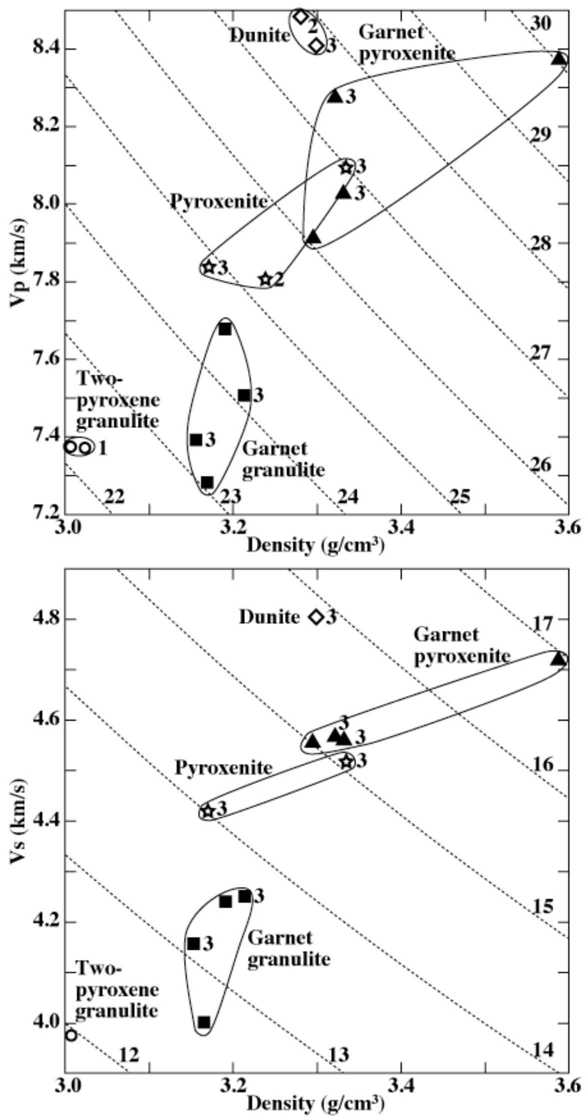

Vp (km/s)
Density (g/cm³)
Dunite
Garnet pyroxenite
Pyroxenite
Two-pyroxene granulite
Garnet granulite
Vs (km/s)

Figure 10

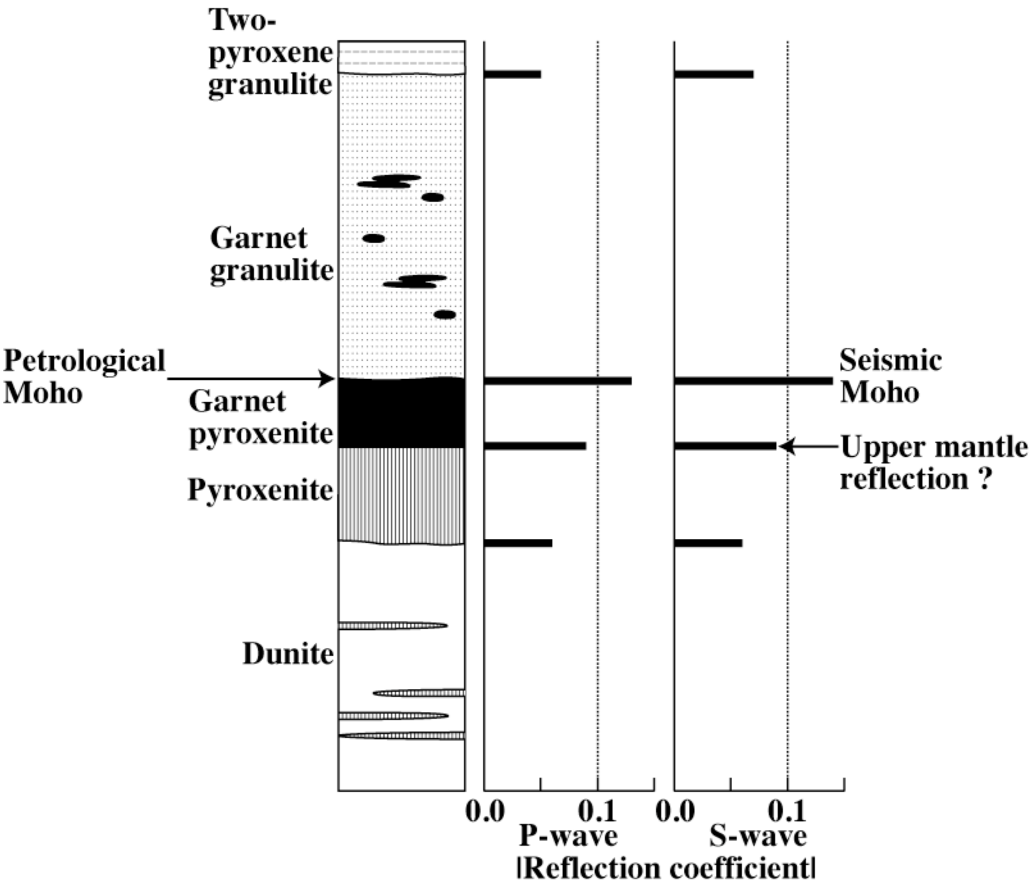
Two-
pyroxene
granulite
Garnet
granulite
Petrological
Moho
Garnet
pyroxenite
Pyroxenite
Dunite
Seismic
Moho
Upper mantle
reflection ?
0.0
0.1
0.0
0.1
P-wave
S-wave
|Reflection coefficient|

Figure 11